

# The Determination of the Crystal Structure of Methyl Melaleucate Iodoacetate

By S. R. HALL\* AND E. N. MASLEN

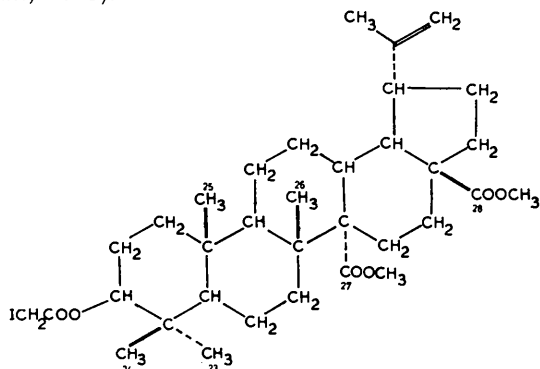
Department of Physics, University of Western Australia, Nedlands, Western Australia

(Received 20 January 1964)

The crystal structure of methyl melaleucate iodoacetate ( $C_{34}H_{51}O_6I$ ), a derivative of melaleucic acid, was determined from phases calculated by anomalous dispersion methods (Ramachandran & Raman, 1956) and refined by block diagonal least squares to a final  $R$  index of 0.079 for 1342 measurable reflexions. The unit cell is orthorhombic, space group  $P2_12_12_1$  with  $a = 15.719$ ,  $b = 24.533$  and  $c = 8.618$  Å. 48 of the 51 H atoms were located in a 3-D difference synthesis enabling a close study of the packing and associated steric hindrance in the structure. Abnormally high C-C bond lengths of up to 1.66 Å are attributed to strain resulting from this hindrance.

## Introduction

Methyl melaleucate iodoacetate is a derivative of melaleucic acid, a plant product isolated along with betulinic acid from the paper-like barks of *Melaleuca raphiophylla* Schau., *M. viminea* Lindl. and *M. cuticularis* Labill. Melaleucic acid was suggested by Arthur, Cole, Thieberg & White (1956) to have the constitution 3 $\beta$ -hydroxylup-20(29)-ene-25,28-dioic acid. Subsequent investigation showed that the more hindered carboxyl group was not at C(25), and with the study of a number of derivatives by nuclear magnetic resonance spectra, Chopra, Fuller, Thieberg, Shaw, White, Hall & Maslen (1963) suggested that it was 3 $\beta$ -hydroxylup-20(29)-ene-27,28-dioic acid. Methyl melaleucate iodoacetate (I) was prepared with the aim of using X-ray diffraction techniques to provide an independent check of the molecular formula and the position of the carboxyl at C(27). Preliminary structure analysis confirming the suggested constitution has already been reported (Chopra *et al.*, 1963).



(I)

Since the derivative contained an iodine atom it was intended to solve the structure by normal heavy-

atom techniques. However, during the collection of intensity data large differences between the intensities of the  $hkl$  and the  $\bar{h}\bar{k}l$  reflexions were observed, indicating the possibility of using anomalous dispersion phasing methods.

Two techniques have been proposed for the solution of structures from anomalous dispersion measurements. They are, the direct phase method suggested by Ramachandran & Raman (1956) and the sine-Patterson methods proposed by Okaya, Saito & Pepinsky (1955). Geurtz, Peerdeman & Bijvoet (1963) have indicated in a comparison of these two methods that the results from the sine-Patterson function are less clear than those of the direct phase method. In view of this and the possible difficulties in deconvoluting the sine-Patterson function, the direct phase method was chosen to solve this structure.

It is interesting to note that the majority of previous structures solved by the direct phase methods such as L(+)-lysine hydrobromide dihydrate (Raman, 1959), Factor Vla (Dale, 1962) and cystine hydrobromide (Geurtz *et al.*, 1963) contained centrally arranged anomalous scatterers which may have presented problems of artificial symmetry if solved by normal methods. However, although no such difficulties arose in the solution of methyl melaleucate, as the iodine is accentrically placed, the direct phase method was chosen as a superior technique.

## Experimental

### Crystal data

Methyl melaleucate iodoacetate ( $C_{34}H_{51}O_6I$ ).  
M.W. 682.7.

$a = 15.719 \pm 5$ ,  $b = 24.533 \pm 7$ ,  $c = 8.618 \pm 5$  Å.  
 $V = 3323.3$  Å<sup>3</sup>.

Space group:  $P2_12_12_1$  ( $D_2^4$ ), acentric with 4 molecules per unit cell.  $F(000) = 1428$  electrons. Crystal form: colourless orthorhombic needles with long axis in  $c$  direction. Crystallized from methanol. Density:

\* Present address: Division of Pure Physics, National Research Council, Ottawa 2, Canada.

measured =  $1.37 \pm 1$ , calculated =  $1.366 \pm 1$ . Linear absorption coefficient for Cu  $K\alpha$ :  $80.7 \text{ cm}^{-1}$ .

#### Intensity data collection

Crystals of methyl melaleucate iodoacetate were supplied by C. Chopra, Department of Chemistry, University of Western Australia, who prepared specimens suitable for X-ray photography by slow crystallization from methanol. The crystals, which are stable at room temperature, were in the form of colourless needles, elongated in the  $c$  direction and of a generally rectangular cross-section. A crystal was mounted about the long axis and a series of photographs was taken with a Buerger precession camera. From these the unit-cell dimensions, corrected for film shrinkage, were measured.

Systematic absences in the  $0k0$ ,  $00l$  and  $h00$  reflexions on these photographs uniquely determined the space group as  $P2_12_12_1 (D_2^5)$ , which is acentric with four equivalent positions per unit cell. The theoretical density, assuming one molecule per asymmetric unit, was calculated as  $1.366 \pm 1$  and this compares favourably with the value of  $1.37 \pm 1$  measured by the flotation method.

Two crystal specimens were prepared for X-ray diffraction studies. The first specimen, which had the approximate dimensions  $0.29 \times 0.27 \times 1.00 \text{ mm}^3$ , was mounted along the  $c$  axis and aligned on an oscillation camera. With Cu  $K\alpha$  radiation ( $1.5418 \text{ \AA}$ ) a series of photographs of the layers  $l=0$  to 7 was then taken by multi-film, multi-exposure equi-inclinal Weissenberg techniques. The intensity data were limited by an apparently high overall temperature factor so that only a few reflexions were observed with Bragg angles ( $\theta$ ) greater than  $50^\circ$ . To ensure the maximum number of measurable reflexions, exposure times of up to 96 hours at 40 kV and 25 mA were necessary. Intensity spot shapes were generally uniform and therefore no spot integration was required.

The second crystal specimen was prepared by slicing a block of dimensions  $0.27 \times 0.25 \times 0.22 \text{ mm}^3$  from a needle crystal and mounting it about the  $a$  axis. Intensity data of layers  $h=0, 1$  and  $2$  were collected with procedures similar to those used for the first specimen.

#### Intensity correlation

The intensities of the  $hkl$  and  $\bar{h}\bar{k}\bar{l}$  reflexions, which are non-equivalent because the iodine atom is an anomalous scatterer to Cu  $K\alpha$  radiation, were measured separately by visual comparison with a calibrated intensity strip. This excluded the  $0kl$ ,  $h0l$  and  $hk0$  reflexions which, since the projections in space group  $P2_12_12_1$  are centric, are equivalent to  $0\bar{k}\bar{l}$ ,  $\bar{h}0\bar{l}$  and  $\bar{h}\bar{k}0$  reflexions and therefore were only measured once. The indexing of the  $hkl$  and  $\bar{h}\bar{k}\bar{l}$  reflexions on the Weissenberg films was carried out by the procedure suggested by Peerdeman & Bijvoet (1956). Only 1342

$hkl$  reflexions of the 3795 theoretically observable independent reflexions in an octant of the Cu  $K\alpha$  sphere were observed. This was primarily because the intensity data did not extend beyond the Bragg angle of  $50^\circ$ .

Lorentz and polarization factors were applied to all reflexions ( $hkl$  and  $\bar{h}\bar{k}\bar{l}$ ) and cylindrical and spherical absorption factors were applied to the  $c$ - and  $a$ -axis data respectively. Although the linear absorption coefficient for Cu  $K\alpha$  is high ( $80.7 \text{ cm}^{-1}$ ), these absorption factors were considered to be a sufficiently accurate approximation for the solution and the initial refinement of the structure. Correlation in the latter stages of refinement showed that errors in these factors were considerably less than the errors in the measurement of the visual intensity data. The application of general absorption factors involving the exact crystal shape was therefore unnecessary.

The observed structure factors were correlated by comparing the common row lines of the  $c$ - and  $a$ -axis layers, in addition to calculating absolute scaling factors by Wilson (1942) plots for each layer. The final layer scales obtained by a combination of these methods proved quite accurate and did not require adjustment during the complete refinement. The comparison of common row lines also provided a convenient check on the indexing of the  $hkl$  and  $\bar{h}\bar{k}\bar{l}$  reflexions. After the application of the layer scales, common row reflexions in the  $c$ - and  $a$ -axis data were consistent to within 7%, the accuracy expected of good visual data.

#### Location of the iodine atom

A Patterson synthesis was calculated for the projection down  $[001]$ . This projection has the plane group symmetry  $pgg$  and vectors between identical atoms related by this symmetry give rise to three peaks per asymmetric unit at  $2x$ ,  $2y$ ;  $\frac{1}{2}$ ,  $\frac{1}{2} - 2y$  and  $\frac{1}{2} - 2x$ ,  $\frac{1}{2}$ . Peaks corresponding to the iodine-iodine vectors were readily identified and the atom was located at

$$x/a = 0.116 \quad \text{and} \quad y/b = 0.203.$$

Similarly a Patterson synthesis calculated for the projection down  $[100]$  gave pronounced peaks corresponding to the iodine positions of  $y/b = 0.204$  and  $z/c = 0.133$ . These coordinates compare reasonably well with the final coordinates of the iodine atom,

$$x/a = 0.1211, \quad y/b = 0.2044 \quad \text{and} \quad z/c = 0.1239,$$

the largest deviation from the initial position being less than  $0.1 \text{ \AA}$ .

#### Solution of the Structure

Structure factor phase determination by anomalous dispersion methods has been developed by Ramachandran & Raman (1956) with special reference to the case of centrally placed heavy atoms. The method

may be presented in a slightly more convenient form, particularly for the solution of structures containing acentrically placed heavy atoms.

The departure from Friedel's Law (1913) is due to an atom in the structure being excited by the incident X-radiation and the resulting diffracted wave having both a real and an imaginary component. These components are usually expressed as corrections to the normal scattering factor  $f^0$ . The total scattering factor may then be written in the form

$$f = f^0 + \Delta f' + i \Delta f'' = f' + i \Delta f''$$

where  $\Delta f'$  is the real and  $\Delta f''$  the imaginary correction to the atomic scattering factor. These corrections give rise to the real and imaginary components  $F'_A$  and  $F''_A$  respectively, in the total structure factor  $F_H$  as seen

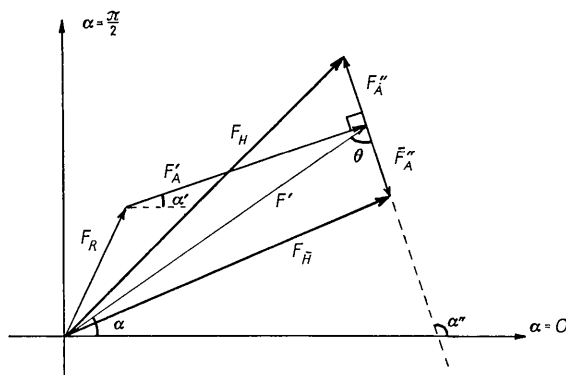


Fig. 1. Structure factor phase diagram for a structure containing one type of acentrically placed anomalous scatterer.

in the phase diagram (Fig. 1). Fortunately the imaginary component provides a means of estimating the mean phase  $\alpha$  without any knowledge of the non-anomalous scatterers (which contribute  $F_R$  in Fig. 1) from the simple relationship

$$\alpha = \alpha'' - \theta \tag{1}$$

where  $\alpha''$  is the phase of  $F''_A$  and  $\theta$  is the difference in phase between  $F'_A$  and  $F''_A$ , the total structure factor without the imaginary component. The phase difference  $\theta$  may be calculated from the trigonometrical expression

$$\cos \theta = \Delta F_o^2 / 4F''_A \cdot |F''_A| \tag{2}$$

where  $\Delta F_o^2$  is the Bijvoet inequality ( $F_{ohkl}^2 - F_{o\bar{h}\bar{k}\bar{l}}^2$ ). The magnitude of  $F'$  may be deduced from

$$F' = \sqrt{\frac{1}{2}(F_{ohkl}^2 + F_{o\bar{h}\bar{k}\bar{l}}^2) - F_A'^2} \tag{3}$$

When only one type of anomalous scatterer is present in the structure, the phase  $\alpha''$  may be replaced by  $\alpha' + \pi/2$ , where  $\alpha'$  is the phase of  $F'_A$ . This latter form is preferable since the errors in  $\alpha'$  should be much smaller than  $\alpha''$  because of the relative magnitudes of the real  $f'$  and the imaginary  $\Delta f''$  components of the atomic scattering factor. If more than

one type of anomalous scatterer is present in the structure  $\alpha''$  may have any value relative to  $\alpha'$ . In this case therefore  $\alpha''$  must be used in equation (1).

The evaluation of  $\theta$  from equation (2) poses an ambiguity in sign which permits the value of the phase  $\alpha$  to be expressed as either  $\alpha_1 = \alpha' + \pi/2 - \theta$  or  $\alpha_2 = \alpha' + \pi/2 + \theta$ . The problem of which phase is the correct one is overcome by choosing the phase closest to the heavy atom phase  $\alpha'$ . Since the anomalous scatterer usually represents a high proportion of the scattering power, this criterion is generally a valid one, the true phase normally lying closer to  $\alpha'$  than to  $\alpha' + \pi$ .

Consider the general case of  $N$  anomalous scatterers acentrically arranged in the unit cell. The components  $F'_A$  and  $F''_A$  may be expressed as

$$F'_A = \sum_{j=1}^N f'_j \cos 2\pi H \cdot x_j + i \sum_{j=1}^N f'_j \sin 2\pi H \cdot x_j \tag{4}$$

$$F''_A = - \sum_{j=1}^N \Delta f''_j \sin 2\pi H \cdot x_j + i \sum_{j=1}^N \Delta f''_j \cos 2\pi H \cdot x_j \tag{5}$$

For the case of one anomalous scatterer only the phase  $\alpha'$  and magnitude  $F'_A$  need be calculated from these equations for the evaluation of the direct phase, though the value of  $F''_A$  is necessary if an  $R$  index is required.

#### Application

The first phase calculations were programmed on an IBM 1620 computer as a modification of F. R. Ahmed's structure factor program (I.U.Cr. *World List of Computer Programs*, 1962). It was necessary in drafting these modifications to incorporate a logical routine to deal with reflexions where inaccuracies in intensity measurement or the anomalous scatterer position give rise to meaningless results when applied to equation (2).

The following criteria were adopted in this logical routine for the treatment of doubtful reflexions.

(i) If  $\cos \theta > 1$ ,  $\theta$  is put equal to zero. This results in the direct phase being put equal to  $\alpha' = \pi/2$ , differing from the heavy atom phase by  $\pi/2$ . Other alternatives to this criterion are either to exclude the reflexion completely or to put the direct phase equal to the heavy atom phase. A series of Fourier synthesis sections were calculated with data in which the unreliable reflexions were treated according to each of the three alternatives. The accepted criterion, putting  $\theta = 0$ , gave the most pronounced peaks at the atomic sites and was therefore chosen as that providing the most reliable phase.

(ii) If  $F'$  or  $F'_A = 0$ ,  $\alpha$  is put equal to  $\alpha'$ .

(iii) If  $2F_A'^2 > F_{ohkl}^2 + F_{o\bar{h}\bar{k}\bar{l}}^2$  in the calculation of  $F'$ ,  $\alpha$  is put equal to  $\alpha'$ . This criterion is only necessary in smaller structures where  $\Sigma f_o$  is of the same order as  $\Sigma \Delta f''$ .

The output of the modified structure factor program was in the form of two sets of components, one set

having the direct phase  $\alpha$  and the other the heavy atom phase  $\alpha'$ . The first set were used to calculate a three-dimensional  $F_o$  Fourier synthesis with sections along the  $c$  axis, since it was expected, from the crystal form, that the molecule would lie roughly parallel to this plane. By superimposing the Fourier sections, the molecule was detected as a region of high density running approximately parallel to the  $a$  axis. A section down the  $z$  direction in the plane of the high density region enabled the basic ring system to be identified and 40 of the 41 non-hydrogen atoms were readily positioned. The peaks at the atomic sites were generally well resolved with peak heights ranging from 3 to 6  $e.\text{\AA}^{-3}$ . As a comparison, sections of the Fourier  $F_o$ -synthesis perpendicular to the  $b$  axis were calculated using both the direct phase and the heavy atom phase. Fig. 2(a) and (c) shows the sections at  $y/b=18/120$  and these illustrate the general superiority of the anomalous dispersion phased synthesis. The former is very similar to the section of the final  $F_o$ -Fourier synthesis (Fig. 2(d)).

Calculation of the structure factor scale ( $\Sigma F_c/\Sigma F_o$ ) earlier had shown that the  $F_o$  values were twice absolute. This error, which occurred during correlation, might have been expected to have significantly affected the calculation of the direct phases, since equation (2) requires that  $F_o$  and  $\Delta F_o^2$  are absolutely scaled. The direct phases were therefore recalculated with the correct scale and another three-dimensional  $F_o$  Fourier synthesis was evaluated. Fig. 2(b) is a section of  $y/b=18/120$  of this synthesis. It appears to be essentially the same as the section calculated with the incorrectly scaled direct phases, except that Fig. 2(a) has slightly more pronounced spurious peaks. It appears therefore that the direct phase is relatively insensitive to errors in the scale of  $F_o$  and  $\Delta F_o^2$ . A possible explanation of this is that the direct phase  $\alpha$  may be considered as corrected by the addition of the factor  $(\pi/2 - \theta)$ . If the scale in the calculation of  $\theta$  is not grossly incorrect, the value of  $\alpha$  will always tend to be closer to the true phase than  $\alpha'$ . Since  $\cos \theta$  which is a slow varying function for small  $\theta$  for the majority of reflexions has a value close to zero, the resulting corrections  $(\pi/2 - \theta)$  are generally small. During the first direct phase calculation the scale and consequently  $\cos \theta$  were in error by a factor of two, resulting in the maximum of number of reflexions *versus* correction factor  $(\pi/2 - \theta)$  occurring at about  $24^\circ$ . When the correct scale was used to calculate  $\theta$ , the equivalent maximum was at about  $13^\circ$ , a difference of only  $11^\circ$  from the former value. Moreover a number of the absurdities resulting from the wrong scale had been rectified by the 'logical routine' procedure of setting  $\theta$  equal to zero when  $\cos \theta$  exceeds one, the number of reflexions with low  $\theta$  is relatively small, and the data of methyl melaleucate contain 552 centric reflexions which necessarily have the heavy atom phase. Fig. 2(a) and (b) might therefore be expected to be fairly similar. On the other hand the

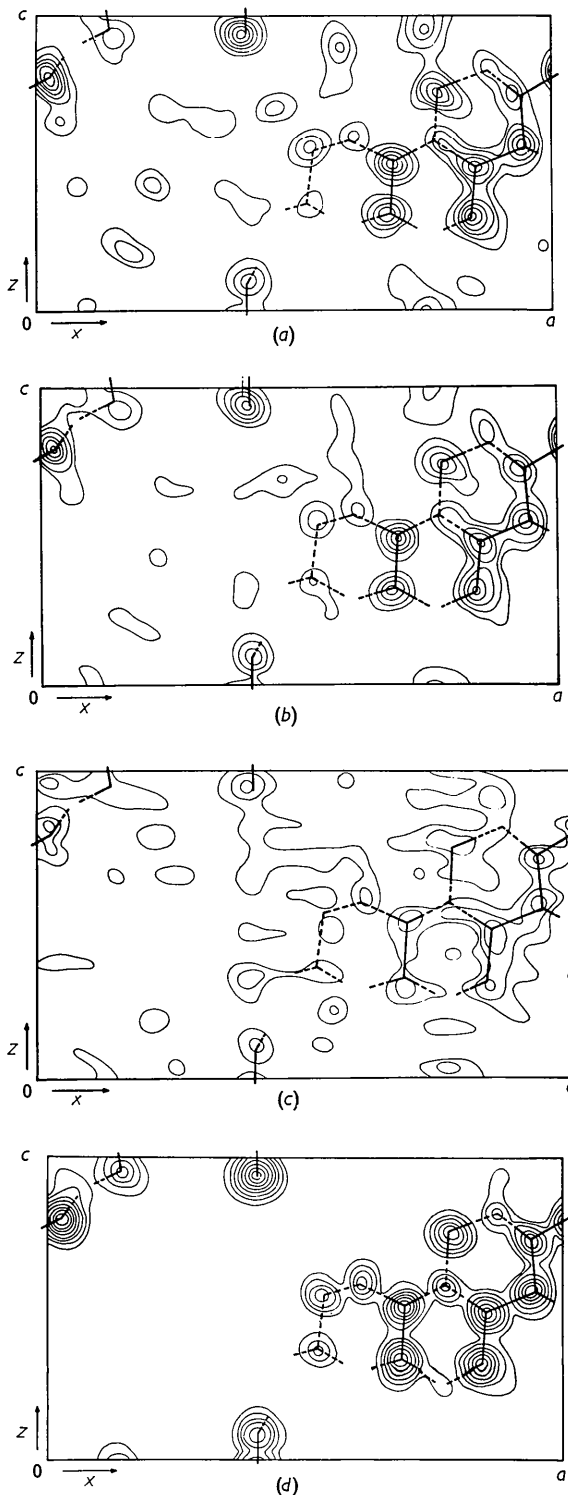


Fig. 2.  $F_o$  Fourier sections at  $y/b=18/120$  from structure factors phased from (a) anomalous dispersion calculations using the incorrect scale, (b) anomalous dispersion calculations using the correct scale, (c) heavy atom structure factor calculation and (d) final structure factor calculation involving all atoms. Contours from 1  $e.\text{\AA}^{-3}$  at intervals of 1  $e.\text{\AA}^{-3}$ .

reflexions which have low  $\theta$ -values, although few in number, provide the greatest difference from the pure heavy atom phasing and as these are considerably in error the degree of correspondence between the maps with the correct and incorrect phases is surprising. There are a number of possible explanations for this anomaly and a detailed analysis of these has been undertaken. The results of this investigation will be reported in a later paper.

Structure factors on all non-hydrogen atoms, except the oxygen atom O(2), were evaluated with a mean isotropic temperature factor coefficient of  $4.9 \text{ \AA}^2$  obtained during the Wilson plot scaling and the atomic scattering factors calculated by Freeman (1959) for oxygen and carbon. The resulting reliability index was 0.24, a drop of 0.14 from the structure factors calculated on the iodine atom alone.

In order to locate the oxygen atom O(2), a three-dimensional difference Fourier synthesis, phased on the other non-hydrogen atoms, was calculated. The oxygen was readily identified on a peak of height  $4 \text{ e.\AA}^{-3}$ . This had a pronounced elliptical shape indicating strong anisotropic thermal motion, which was confirmed by the subsequent refinement. Its high temperature factor probably accounts for the difficulty in locating this atom in the initial Fourier synthesis. The three-dimensional difference synthesis also enabled coordinate and temperature factor corrections to be made on most other atoms, especially the iodine where there was also strong evidence for thermal anisotropy.

Another round of structure factors was calculated, an anisotropic temperature factor being given to the iodine and isotropic temperature factors to all other non-hydrogen atoms. The resulting  $R$  value of 0.19 indicated that the structure was basically correct.

### Refinement of the structure

Depending on the accuracy and the size of the structure, one of two methods may be adopted in the calculation of the structure factors of a structure containing anomalous scatterers. The first, for use with accurate data, involves all the structure factor components, real and imaginary, in the calculation. The second method is an approximation which disregards the contribution of the imaginary correction to the scattering factor and is more appropriate for the refinement of a large structure with visual data.

The first method involves the general structure factor equations

$$F_{hkl} = F_H = \sum_{j=1}^N (f_j' + i\Delta f_j'') \exp(2\pi i H \cdot x_j) + \sum_{j=1}^M f_j^0 \exp(2\pi i H \cdot x_j) \quad (6)$$

and

$$F_{\bar{h}\bar{k}\bar{l}} = F_{\bar{H}} = \sum_{j=1}^N (f_j' + i\Delta f_j'') \exp(-2\pi i H \cdot x_j) + \sum_{j=1}^M f_j^0 \exp(-2\pi i H \cdot x_j) \quad (7)$$

where  $N$  is the number of anomalous and  $M$  the number of non-anomalous scatterers per unit cell. During refinement normally only one set of observed structure factors ( $F_{oH}$ ) is compared with the values calculated from equation (6), but it is also possible to use both  $F_{oH}$  and  $F_{o\bar{H}}$  since this is effectively equivalent to having two sets of independently measured data. Although this increases the length of the structure factor calculation, the reliability of the structure determination will be improved.

In the second method, the imaginary component is ignored. Equation (6) therefore simplifies to

$$F_H' = \sum_{j=1}^N f_j' \exp(2\pi i H \cdot x_j) + \sum_{j=1}^M f_j^0 \exp(2\pi i H \cdot x_j) \quad (8)$$

In the refinement  $F_H'$  is compared with the mean observed structure factor  $F_{oM}$  which is derived from  $\sqrt{(F_{oH}^2 + F_{o\bar{H}}^2)/2}$ . The equivalence of  $F_H'$  and  $F_{oM}$  follows since  $F_H'$  is the calculated version of  $F'$  from equation (3), and this is equal to  $F_{oM}$  if the imaginary component  $F_A''$  is small in comparison. The condition that  $F_A''$  is small holds for large structures where  $\Sigma \Delta f_j''$  is small compared with  $\Sigma f_j^0$  and  $\Sigma f_j'$ .

The structure factors for methyl melaleucate iodoacetate were therefore evaluated by the use of equation (8). In the following text the calculated and observed structure factors refer to  $F_H'$  and  $F_{oM}$  respectively.

The structure was refined mainly by least-squares methods (Hughes, 1941), though a number of Fourier

Table 1. *Progress of structure refinement*

$R$  = Reliability index  $M = \Sigma w(F_o - F_c)^2 \times 10^{-2}$

2-D Patterson synthesis* down [001] and [100]
Direct phase SF calculation ( $R=0.38$ )
Direct phase $F_o$ Fourier synthesis
SF calculation ( $R=0.24$ ), 40 non-hydrogen atoms
Difference Fourier synthesis. Location of atom O(2)
SFLS (1) calculation ( $R=0.19$ ; $M=285$ ), 41 non-H atoms
SFLS (2) calculation ( $R=0.18$ ; $M=177$ ), 41 non-H atoms
SFLS (3) calculation ( $R=0.13$ ; $M=130$ )
SFLS (4) calculation ( $R=0.123$ ; $M=91$ )
Empirical secondary extinction corrections ( $R=0.114$ )
SFLS (5) calculation ( $R=0.104$ ; $M=74$ )
Difference Fourier synthesis. Location of hydrogen atoms
SFLS (6) calculation ( $R=0.093$ ; $M=68$ ), 41 non-H atoms and 51 H atoms (SF only)
SFLS (7) calculation ( $R=0.084$ ; $M=50$ )
SFLS (8) calculation ( $R=0.081$ ; $M=45$ )
SFLS (9) calculation ( $R=0.080$ ; $M=43$ )
SFLS (10) calculation ( $R=0.079$ ; $M=41$ )
SFLS (11) calculation ( $R=0.079$ ; $M=40$ )
SF calculation ( $R=0.079$ )

\* This calculation was carried out on the SILLIAC Computer, University of Sydney. All subsequent calculations were performed on an I.B.M. 1620 computer, University of Western Australia.

and difference syntheses were calculated in the course of refinement. The progress of refinement is shown in Table 1. A block diagonal approximation of the least-squares matrix was used in the solution of the normal equations because of the limited computing facilities available. A least-squares program written by G. A. Mair, of The Royal Institution, London, allowed the simultaneous refinement of the positional parameters and the isotropic and anisotropic temperature factors. Each reflexion was weighted in this calculation by the scheme,

$$\sqrt{w} = 1/\sqrt{1 + ((F_o - b)/a)^2}$$

which was suggested by Mills & Rollett (1960). This gave maximum weight to the terms for which  $|F_o - F_c|$  was least. The values of  $a$  and  $b$  were calculated for each round of least squares by plotting  $\sqrt{((F_o - F_c)^2 - 1)}$  versus  $F_o$ .

All 41 of the non-hydrogen atoms except iodine were initially refined with isotropic temperature factor coefficients. In later rounds, atoms which showed high and diverging values were then assigned an-

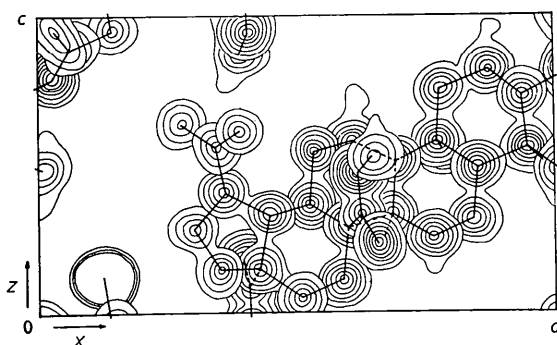


Fig. 3. Composite electron density map projected along the  $b$  axis. Contours are from  $1 \text{ e.}\text{\AA}^{-3}$  at intervals of  $1 \text{ e.}\text{\AA}^{-3}$ .

isotropic coefficients. All atoms listed in Table 2(b), except the iodine atom, showed this behaviour during the refinement. It is interesting to note that all these atoms are in positions in the molecule which give them a relatively high degree of freedom.

#### Secondary extinction

After four rounds of least-squares refinement the observed and calculated structure factors were compared individually. The high values of  $F_c$  were generally larger than the corresponding  $F_o$ 's, suggesting that these reflexions were subject to secondary extinction. A graphical plot of  $\log_e(I_c/I_o)$  versus  $I_c$  confirmed this, showing a consistent relationship between  $I_c$  and  $I_c/I_o$ . Since the crystal used in collecting these intensity data was roughly cylindrical an attempt was made to relate the degree of secondary extinction to the Bragg angle  $\theta$ , as suggested by Hamilton (1957). The presence of a general coefficient  $\epsilon$  was evident though no consistent variation

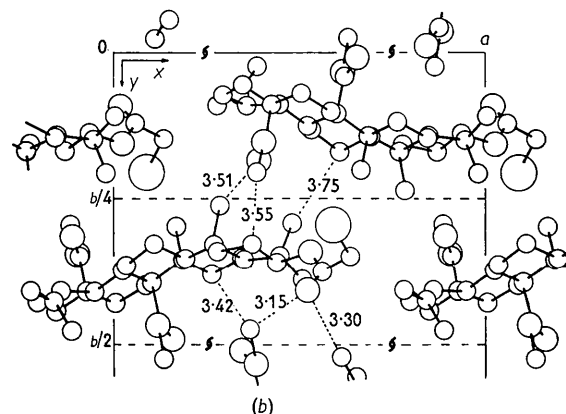
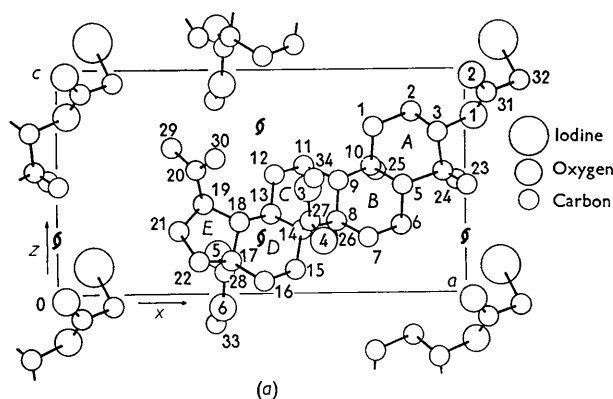


Fig. 4. The structure of methyl melaleucate iodoacetate excluding all hydrogen atoms, (a) projected down the  $b$  axis, (b) projected down the  $c$  axis.

of  $\epsilon$  with  $\theta$  was detected. The value of  $\epsilon$  was estimated by a least-squares calculation including all reflexions above a minimum  $I_o$  value, weighted according to  $I_c$ . As a check on this calculation, values of  $I_c$  and  $\log_e(I_c/I_o)$  were averaged for about 30 discrete ranges of  $I_c$  and plotted manually. Results from both these methods were in good agreement, the final value of  $\epsilon$  being  $1.1 \times 10^{-5}$ . Correction of the observed structure factors using the equation  $F_o^2 = F_{o1}^2 \exp(\epsilon \cdot I_c)$ , where  $F_o$  and  $F_{o1}$  are the corrected and uncorrected observed structure factors respectively, improved the agreement of the stronger reflexions and lowered the overall  $R$  value by 0.01.

#### Location of hydrogen atoms

After another round of least-squares refinement with the data corrected for secondary extinction, there were still a number of marked discrepancies in the low order terms. This was expected to result from contribution of the hydrogen atoms. A three-dimensional difference synthesis was calculated in an attempt to locate the 51 hydrogen atoms in the structure. 34 of the 51 can be approximately positioned from the knowledge of the basic skeleton, 28 being

Table 2(a). Coordinates and isotropic thermal parameters of the non-hydrogen atoms

I	$x/a$	$y/b$	$z/c$	$B$		$x/a$	$y/b$	$z/c$	$B$
I	0.1211	0.2044	0.1239		C(15)	0.5849	0.1016	0.1042	3.2
O(1)	0.0244	0.1556	0.7913	5.0	C(16)	0.5076	0.0701	0.0528	5.6
O(2)	0.0267	0.0856	0.9582		C(17)	0.4282	0.0896	0.1501	3.5
O(3)	0.6165	0.0333	0.4691	4.2	C(18)	0.4475	0.0865	0.3256	3.1
O(4)	0.6553	0.0113	0.2306	5.3	C(19)	0.3597	0.0954	0.4019	4.5
O(5)	0.3951	0.1869	0.1755	5.0	C(20)	0.3403	0.0714	0.5590	5.6
O(6)	0.4054	0.1510	-0.0596	5.4	C(21)	0.2995	0.0703	0.2782	6.7
C(1)	0.7814	0.1572	0.7514	4.3	C(22)	0.3501	0.0556	0.1420	4.5
C(2)	0.8705	0.1692	0.8137	4.8	C(23)	0.0045	0.1088	0.4830	4.7
C(3)	0.9352	0.1388	0.7278	4.0	C(24)	0.9798	0.2073	0.5133	5.0
C(4)	0.9475	0.1493	0.5559	2.6	C(25)	0.7835	0.2337	0.5544	3.6
C(5)	0.8503	0.1415	0.4881	2.5	C(26)	0.6690	0.1994	0.2487	4.0
C(6)	0.8427	0.1456	0.3101	4.1	C(27)	0.6245	0.0434	0.3272	5.7
C(7)	0.7650	0.1187	0.2549	2.9	C(28)	0.4061	0.1469	0.0903	5.5
C(8)	0.6842	0.1428	0.3276	2.2	C(29)	0.2760	0.0919	0.6342	
C(9)	0.6926	0.1457	0.5046	1.7	C(30)	0.3880	0.0252	0.6126	
C(10)	0.7723	0.1695	0.5732	2.6	C(31)	0.0577	0.1230	0.8911	7.8
C(11)	0.6097	0.1684	0.5769	3.7	C(32)	0.1380	0.1473	0.9519	
C(12)	0.5330	0.1318	0.5412	2.7	C(33)	0.3917	0.2053	-0.1270	
C(13)	0.5214	0.1244	0.3662	3.1	C(34)	0.6440	-0.0215	0.5246	
C(14)	0.6017	0.1035	0.2830	3.0					

Table 2(b). Anisotropic thermal parameters

I	$\beta_{11}$	$\beta_{22}$	$\beta_{33}$	$\beta_{23}$	$\beta_{13}$	$\beta_{12}$
O(2)	0.00833	0.00420	0.01664	-0.00080	-0.00007	-0.00116
C(29)	0.01094	0.00593	0.07849	0.02575	-0.04645	-0.00868
C(30)	0.01365	0.00456	0.02805	-0.00311	0.01406	0.00103
C(31)	0.00702	0.00327	0.02283	0.00550	0.00188	-0.00312
C(32)	0.00607	0.00442	0.02419	-0.00770	-0.00714	-0.00331
C(33)	0.01002	0.00214	0.02502	0.00732	-0.00466	0.00189
C(34)	0.01945	0.00096	0.02673	0.00075	-0.01761	0.00661

tetrahedrally bonded to the basic ring system and another 6 existing in a *gem*-dimethyl configuration. These are referred to below as group I hydrogen atoms. Of the remaining 17, 15 were in five methyl groups and their positions are restricted to the circumference of a circle of radius 1.03 Å centred at the intersection of the produced C-C bond and a plane perpendicular to it. The other two hydrogen atoms H(50) and H(51) in the vinylidene group have their positions restricted to a plane containing the C(20)-C(29) double bond. These 17 atoms will be referred to below as the group II hydrogen atoms.

The group I hydrogen positions were calculated assuming the carbon-hydrogen bond distance of

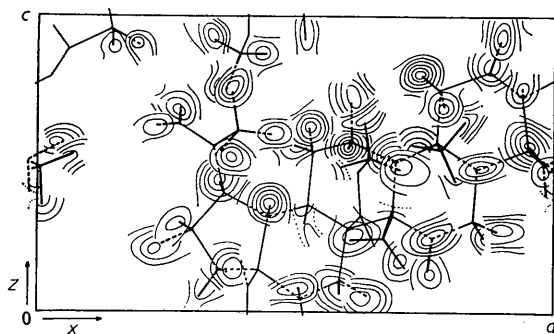


Fig. 5. A summary of a three-dimensional difference synthesis projected along the  $b$  axis to locate the hydrogen atoms. Contours from 0.1  $e.\text{\AA}^{-3}$  at intervals of 0.1  $e.\text{\AA}^{-3}$ .

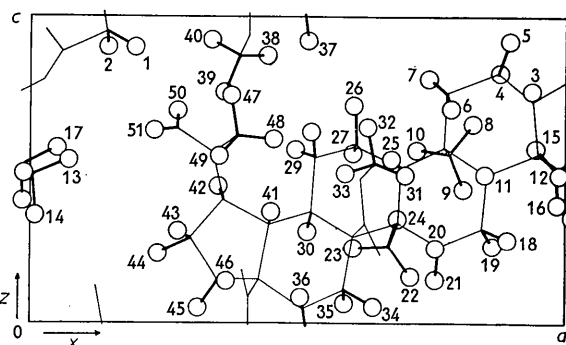


Fig. 6. Diagrammatic representation of the structure showing the hydrogen atoms as positioned from the difference synthesis (see Fig. 5).

1.09 Å and an ideal tetrahedral configuration. As shown in Fig. 5, a summary of the three-dimensional difference synthesis, most atoms of this group were clearly indicated by positive peaks or areas, ranging from 0.1 to 0.7  $e.\text{\AA}^{-3}$ . Exceptions were atoms H(16) and H(30) which were in negative regions. These two atoms were positioned purely from stereochemical considerations, while the positions of the other hydrogens are a compromise between the shape of the positive regions in the difference synthesis and the calculated tetrahedral sites. The atomic coordinates of the group I hydrogen atoms are indicated by an asterisk in Table 4.











coordinates. All atoms were included in a final round of least-squares refinement. Although the shifts on all atoms were less than 0.25 of the estimated standard deviations, they were applied to the coordinates and a final round of structure factors was calculated.

Since the calculated shifts had become insignificant with respect to the estimated standard deviations and the value of  $\sum w(F_o - F_c)^2$ , which is listed in Table 1, had reached a satisfactory minimum of  $40 \times 10^2 e^2$  it was considered that the structure had been refined to the limit of the data. The final *R* value was 0.079.

## Discussion

### General

As reported earlier (Chopra *et al.*, 1963) the structure of methyl melaleucate iodoacetate has confirmed the constitution of melaleucic acid as  $3\beta$ -hydroxyup-20(29)-ene-27,28-dioic acid.

The final reliability index of the structure is 0.079 for 1342 observed reflexions, which is consistent with the accuracy of 0.07 estimated during correlation of common row lines of two separate sets of data. The general accuracy of the structure was enhanced by the use of both *hkl* and  $\bar{h}\bar{k}\bar{l}$  reflexions in estimating the observed structure factors.

### Bond lengths and angles

The bond lengths and angles, calculated from the atomic coordinates given in Table 2, together with the appropriate standard deviations, are listed in Tables 5 and 6. The standard deviations are estimated by the use of Cruickshank & Robertson's (1953) formulae.

Several carbon-carbon bonds and C-C-C angles deviate by more than  $3\sigma$  from the accepted values

Table 5. Bond lengths of covalent bonds between non-hydrogen atoms

Bond	Length (Å)	e.s.d. (Å)	Bond	Length (Å)	e.s.d. (Å)
I-C(32)	2.058	0.027	C (7)-C (8)	1.534	0.023
O (2)-C(31)	1.189	0.039	C (8)-C (9)	1.532	0.020
C(30)-C(20)	1.435	0.034	C (8)-C(14)	1.660	0.022
C(29)-C(20)	1.301	0.043	C (8)-C(26)	1.365	0.025
C(32)-C(31)	1.491	0.039	C (9)-C(10)	1.503	0.022
C(33)-O (6)	1.469	0.027	C (9)-C(11)	1.548	0.024
C(34)-O (3)	1.490	0.026	C(10)-C(25)	1.593	0.023
O (1)-C (3)	1.560	0.027	C(11)-C(12)	1.534	0.025
O (1)-C(31)	1.285	0.032	C(12)-C(13)	1.529	0.024
O (3)-C(27)	1.254	0.025	C(13)-C(14)	1.539	0.023
O (4)-C(27)	1.244	0.026	C(13)-C(18)	1.528	0.024
O (5)-C(28)	1.237	0.026	C(14)-C(15)	1.564	0.023
O (6)-C(28)	1.295	0.026	C(14)-C(27)	1.565	0.027
C (1)-C (2)	1.528	0.026	C(15)-C(16)	1.506	0.029
C (1)-C(10)	1.571	0.026	C(16)-C(17)	1.578	0.030
C (3)-C (4)	1.516	0.029	C(17)-C(18)	1.544	0.023
C (3)-C (2)	1.461	0.027	C(17)-C(22)	1.487	0.026
C (4)-C (5)	1.646	0.025	C(17)-C(28)	1.535	0.028
C (4)-C(23)	1.479	0.029	C(18)-C(19)	1.544	0.026
C (4)-C(24)	1.553	0.029	C(19)-C(20)	1.507	0.031
C (5)-C (6)	1.542	0.026	C(19)-C(21)	1.552	0.033
C (5)-C(10)	1.585	0.023	C(21)-C(22)	1.463	0.034
C (6)-C (7)	1.467	0.026			

of  $1.54 \pm 3$  Å and  $109.3^\circ$ , particularly the C(4)-C(5) and C(8)-C(14) bonds of 1.64 and 1.66 Å and the angles C(4)-C(3)-O(1); C(2)-C(3)-C(4) and C(4)-C(5)-C(10) of  $100.5^\circ$ ,  $119.8^\circ$  and  $120.2^\circ$  respectively.

Two factors appear to be responsible for these deviations. They are the degree of substitution at the carbon atoms in the bonds and the presence of long range steric strain in the structure. Each of these points will be considered in turn.

It seems significant that all the long C-C bonds are attached to at least one of the five fully substituted carbon atoms C(4), C(10), C(8), C(14) and

Table 6. Bond angles for covalent bonds between non-hydrogen atoms

Angle	e.s.d.	Angle	e.s.d.	Angle	e.s.d.			
I-C(32)-C(31)	114.6°	1.8°	C(4)-C(8)-C(26)	107.1°	1.2°	C(16)-C(17)-C(28)	106.1°	1.5°
C(3)-O(1)-C(31)	115.9	1.7	C(8)-C(9)-C(10)	118.7	1.2	C(18)-C(17)-C(22)	100.3	1.4
C(33)-O(6)-C(28)	117.7	1.9	C(8)-C(9)-C(11)	110.1	1.2	C(18)-C(17)-C(28)	114.7	1.5
C(34)-O(3)-C(27)	117.5	1.7	C(10)-C(9)-C(11)	113.8	1.2	C(22)-C(17)-C(28)	108.1	1.5
C(2)-C(1)-C(10)	112.9	1.5	C(1)-C(10)-C(5)	107.3	1.3	C(13)-C(18)-C(17)	110.0	1.4
O(1)-C(3)-C(4)	100.5	1.5	C(1)-C(10)-C(9)	112.7	1.3	C(13)-C(18)-C(19)	119.7	1.4
O(1)-C(3)-C(2)	108.2	1.5	C(1)-C(10)-C(25)	106.1	1.3	C(17)-C(18)-C(19)	103.5	1.4
C(4)-C(3)-C(2)	119.8	1.7	C(5)-C(10)-C(9)	107.1	1.2	C(18)-C(19)-C(20)	120.5	1.6
C(3)-C(4)-C(5)	102.0	1.5	C(5)-C(10)-C(25)	107.2	1.3	C(18)-C(19)-C(21)	101.3	1.6
C(3)-C(4)-C(23)	112.2	1.7	C(9)-C(10)-C(25)	115.8	1.3	C(20)-C(19)-C(21)	109.8	1.7
C(3)-C(4)-C(24)	115.3	1.6	C(9)-C(11)-C(12)	111.7	1.3	C(29)-C(20)-C(30)	123.4	2.5
C(5)-C(4)-C(23)	109.4	1.5	C(11)-C(12)-C(13)	111.1	1.3	C(30)-C(20)-C(19)	119.4	2.0
C(5)-C(4)-C(24)	109.0	1.5	C(12)-C(13)-C(14)	113.6	1.3	C(29)-C(20)-C(19)	116.9	2.3
C(3)-C(4)-C(24)	108.4	1.6	C(12)-C(13)-C(18)	112.8	1.4	C(19)-C(21)-C(22)	108.5	1.9
C(1)-C(2)-C(3)	111.2	1.5	C(14)-C(13)-C(18)	108.3	1.3	C(17)-C(22)-C(21)	105.7	1.7
C(4)-C(5)-C(6)	114.6	1.4	C(8)-C(14)-C(13)	109.8	1.2	O(3)-C(27)-O(4)	124.4	1.9
C(4)-C(5)-C(10)	120.2	1.3	C(8)-C(14)-C(15)	112.1	1.2	O(3)-C(27)-C(14)	113.6	1.7
C(6)-C(5)-C(10)	111.8	1.3	C(8)-C(14)-C(27)	108.1	1.3	O(4)-C(27)-C(14)	121.5	1.8
C(5)-C(6)-C(7)	110.9	1.5	C(13)-C(14)-C(15)	109.3	1.3	O(5)-C(28)-O(6)	121.9	1.8
C(6)-C(7)-C(8)	112.5	1.4	C(13)-C(14)-C(27)	112.8	1.4	O(5)-C(28)-C(17)	123.8	1.8
C(7)-C(8)-C(9)	110.6	1.2	C(15)-C(14)-C(27)	104.4	1.3	O(6)-C(28)-C(17)	114.0	1.8
C(7)-C(8)-C(14)	109.1	1.2	C(14)-C(15)-C(16)	116.2	1.5	O(2)-C(31)-C(32)	118.9	2.8
C(7)-C(8)-C(26)	106.9	1.3	C(15)-C(16)-C(17)	109.1	1.7	O(2)-C(31)-O(1)	129.6	2.7
C(9)-C(8)-C(14)	108.9	1.2	C(16)-C(17)-C(18)	110.4	1.5	C(32)-C(31)-O(1)	109.3	2.2
C(9)-C(8)-C(26)	113.8	1.3	C(16)-C(17)-C(22)	117.2	1.6			

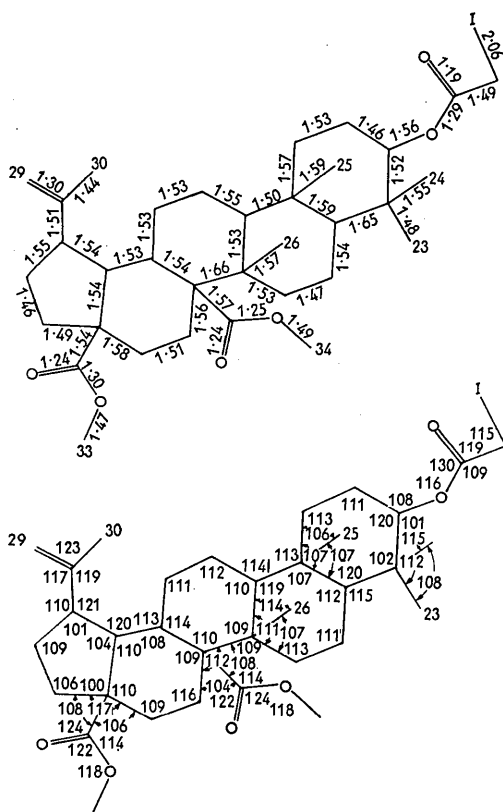


Fig. 7. The structure showing bond lengths (Å) and bond angles (°) between non-hydrogen atoms.

C(17), that the longest bond C(8)–C(14), is the only one which joins two such atoms. The degree of substitution at the bonding carbon atoms appears therefore to bear some relationship to the length of the C–C bond. The exact influence of substitution on bonding is not clear but it would appear that the increase in the number of  $sp^2$ – $sp^3$  bonds in the environment of the C–C bond is associated with the weakening. The usual explanation of this lengthening which has also been observed in hexamethylethane (Bauer & Beach, 1942) is steric repulsion rather than any direct effect on the state of hybridization of the substituent atom.

The second possible factor which may account for the bond and angle deviations is the presence of long range steric strain in the molecule. This type of strain is evident in both the general ‘bowing’ of the basic plane of the ring system which is illustrated in Fig. 4(b), and the obvious distortion of the *A* ring (Fig. 4(a)). There appear to be three sources of long range strain in the structure.

The first is a strain on the ring system due to the steric interaction between the three methyl groups at C(24), C(25) and C(26) which are attached to atoms C(4), C(10) and C(8). As the van der Waals radius for a methyl group is about 2.0 Å and the C(24)⋯C(25) and C(25)⋯C(26) distances are 3.17 and 3.30 Å

respectively, it is evident that, even with the hydrogen atoms in the least hindered positions, there will be considerable interaction in this region. The degree of interaction may be gauged by comparing the inter-methyl carbon distances with the C(10)⋯C(8) contact of 2.59 Å which at first sight appears as if it would be equivalent. The separation of C(24) and C(25) as a result of steric repulsion would tend to flatten the *A* ring at C(4) and C(10), accounting for the large angles C(2)–C(3)–C(4), C(4)–C(5)–C(10) and C(10)–C(1)–C(2) of 119.8°, 120.2° and 112.9° respectively. The hindrance of C(26) would also explain the large angles C(10)–C(9)–C(8) and C(8)–C(7)–C(6) of 118.7° and 112.5°, though as discussed later, these deviations are probably due to another source of strain. With the presence of tensile strain between C(4) and C(10) a slight lengthening of the bonds would be expected, but this alone is unlikely to account for the deviations of 0.1 Å. It is more probable that the distortion from the ideal tetrahedral configuration has resulted in a general weakening of the adjacent bonds similar to that described by Pauling (1960). The decrease in bond strength presumably accounts for the additional lengthening of the bonds C(4)–C(5) and C(5)–C(10) and the subsequent reduction of the angles C(3)–C(4)–C(5) and C(5)–C(10)–C(1). It is interesting to note that the shorter bonds C(2)–C(3) and C(6)–C(7) are consistent with the strain in the *A* and *B* rings resulting in a compressional force on these bonds. Also in agreement with the concept that distorted bond angles result in weaker bonds, the bonds of the three hindered methyl groups to the ring system, C(4)–C(24), C(10)–C(25) and C(8)–C(26) are all longer than normal.

The second source of strain arises from the attachment of the five-membered *E* ring to the six-membered *D* ring. The degree and direction of steric strain resulting from this junction is difficult to assess but from a Drieding model of the structure it seems likely that this could account for the short C(17)–C(22) and C(22)–C(21) bonds of 1.49 and 1.46 Å. This may also cause the *D* ring to be distorted, the puckering being centred at the carbon C(14) on the junction with the *C* ring. The strain and distortion at this point may well contribute to the lengthening of the C(8)–C(14) bond to 1.66 Å and this together with the degree of substitution in the environment of the bond may account for this large deviation. This source of strain, rather than the methyl interaction, appears therefore to be responsible for the large angles of C(10)–C(9)–C(8) and C(14)–C(15)–C(16).

The third source of strain is due to the attachment of the iodoacetate group to the carbon C(3) in the basic ring system. The presence of this strain, which appears to be due to inter- rather than intra-molecular forces, is evident from the low C(4)–C(3)–O(1) angle of 100.5°. The distortion of C(3)–O(1) from the ideal tetrahedron may well explain the elongation of this bond to 1.56 Å. It is interesting to note that a similar

attachment in the structure of epiliminol iodoacetate (Arnott, Davie, Robertson, Sim & Watson, 1961) has comparable C–O and C–C–O values of 1.59 Å and 102° respectively. It is unlikely in methyl melaleucate iodoacetate that the flattening of the A ring will significantly affect the value of the C(4)–C(3)–O(1) angle so the distortion can only be explained in terms of packing forces.

It generally appears then that the longer C–C bonds are dependent on both the degree of substitution in the bonded carbons and the effect of long range steric strain on the bond, whereas the shorter C–C bonds and the abnormal C–C–C angles are only due to the strain.

In the isopropenyl side chain the C(20)–C(29) double bond of 1.30 Å and the C(20)–C(30) single bond of 1.44 Å compare reasonably with the values of 1.33 and 1.50 Å in propylene (Lide & Christensen, 1962). The bond lengths and angles in the two methoxycarbonyl groups are generally consistent with one another and do not differ significantly from values in methyl acetate and methyl chloroformate (O'Gorman, Shand & Schomaker, 1950) and dimethyl oxalate (Dougill & Jeffrey, 1953).

The shorter intermolecular distances shown in Fig. 4(b) are consistent with van der Waals contacts.

#### Hydrogen atom positions

The atomic coordinates of the hydrogen atoms are listed in Table 3, and Fig. 6 shows diagrammatically the positions of these atoms in the unit cell, viewed down the *b* axis.

All group I hydrogen atoms except H(16) and H(30) are close to their expected atomic sites. The group II hydrogen atoms are of more interest since their positions are governed by the intramolecular packing. Fig. 8 shows the positions of the methyl hydrogen atoms attached to C(24), C(25) and C(26) with the van der Waals radius of 1.0 Å. The staggered configuration of these hydrogens appears to be deter-

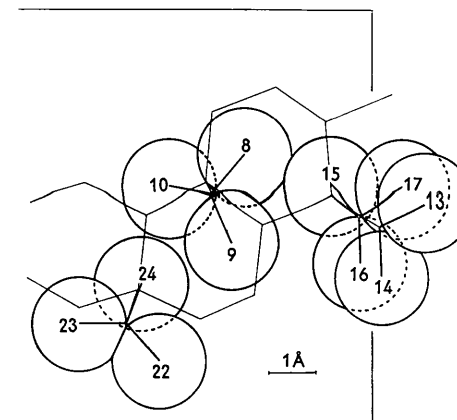


Fig. 8. Part of the structure showing the hydrogen atoms attached to C(23), C(24), C(25) and C(26) with a van der Waals radius of 1.0 Å.

mined by the condition of minimum hindrance to one another, though the orientation of the hydrogen atoms attached to the axial *gem*-dimethyl carbon atom C(24) is also affected by the adjacent equatorial methyl group. It is interesting to note that the positions of the methyl hydrogen atoms attached to C(25) and C(26) are independent of packing with the adjacent ring system, and this contrasts with arrangements often found in unhindered methyl groups.

Hydrogen atoms in the methoxycarbonyl groups at C(33) and C(34) are oriented for minimum hindrance with the adjacent oxygen atoms O(5) and O(4). As the methyl and oxygen van der Waals radii are 2.0 and 1.4 Å and the C(34)···O(4) and C(33)···O(5) distances are 2.66 and 2.65 Å, it would be expected that the close-packing between these atoms is the controlling factor in the orientation of the methoxyl hydrogen atoms. The hydrogen atom sites are consistent with this idea.

The orientation of the isopropenyl side chain with respect to C(20) appears to depend on the hydrogen atom packing with the surrounding atoms. Moreover positions of the hydrogen atoms attached to the C(30) methyl and the C(29) vinylidene carbon atoms within the group are also determined by this packing.

The authors wish to thank C. Chopra for supplying the crystals of methyl melaleucate iodoacetate, members of the Chemistry Department of this University, particularly Prof. D. E. White and Dr A. R. Cole, for their constructive criticism, and Prof. D. H. R. Barton of the University of London for his helpful suggestions. One of us (S. R. H.) wishes to acknowledge the receipt of a Commonwealth Postgraduate Award during this research.

#### References

- ARNOTT, S., DAVIE, A. W., ROBERTSON, J. M., SIM, G. A. & WATSON, D. G. (1961). *J. Chem. Soc.* p. 4183.  
 ARTHUR, H. R., COLE, A. R. H., THIEBERG, K. J. L. & WHITE, D. E. (1956). *Chem. and Ind.* p. 926.  
 BAUER, S. H. & BEACH, J. Y. (1942). *J. Amer. Chem. Soc.* **64**, 1142.  
 CHOPRA, C. S., FULLER, M. W., THIEBERG, K. J. L., SHAW, D. C., WHITE, D. E., HALL, S. R. & MASLEN, E. N. (1963). *Tetrahedron Letters*, **27**, 1847.  
 CRUICKSHANK, D. W. J. & ROBERTSON, A. P. (1953) *Acta Cryst.* **6**, 698.  
 DALE, D. (1962) Ph. D. Thesis. Oxford Univ.  
 DOUGILL, M. W. & JEFFREY, G. A. (1953). *Acta Cryst.* **6**, 831.  
 FREEMAN, A. J. (1959). *Acta Cryst.* **12**, 261.  
 FRIEDEL, G. (1913). *C. R. Acad. Sci., Paris*, **157**, 1533.  
 GEURTZ, J. H., PEERDEMAN, A. F. & BIJVOET, J. M. (1963). *Acta Cryst.* **16**, A 6.  
 HAMILTON, W. C. (1957). *Acta Cryst.* **10**, 629.  
 HUGHES, E. W. (1941). *J. Amer. Chem. Soc.* **63**, 1737.  
 LIDE, D. R. & CHRISTENSEN, D. (1962). *J. Chem. Phys.* **35**, 1374.  
 MILLS, O. S. & ROLLETT, J. S. (1960). *Computing Methods and the Phase Problem in X-ray Crystal Analysis*. London: Pergamon Press.

- O'GORMAN, J. M., SHAND, W. & SCHOMAKER, V. (1950). *J. Amer. Chem. Soc.* **72**, 4222.  
 OKAYA, Y., SAITO, Y. & PEPINSKY, R. (1955). *Phys. Rev.* **98**, 1857.  
 PAULING, L. (1960). *The Nature of the Chemical Bond*. Ithaca: Cornell Univ. Press.  
 PEERDEMAN, A. F. & BIJVOET, J. M. (1956). *Acta Cryst.* **9**, 1012.  
 RAMACHANDRAN, G. N. & RAMAN, S. (1956). *Curr. Sci.* **25**, 348.  
 RAMAN, S. (1959). *Z. Kristallogr.* **111**, 301.  
 WILSON, A. J. C. (1942). **150**, 152.

*Acta Cryst.* (1965). **18**, 279

## Interferometric Studies on Very Pure Silicon Carbide Crystals

BY F. ARRESE

*Royal Holloway College, University of London, Egham, Surrey, England*

(Received 6 January 1964)

Optical multiple-beam interferometric studies are reported for over one hundred extremely pure, clear, colourless, transparent silicon carbide crystals. With one exception they are thin, effectively parallel-sided plates, having surfaces of very high interferometric quality. Most surfaces show regular steps or curvature and these may be due to slip and to buckling after cooling.

The spiral growths so common on the less pure common quality commercial silicon carbide crystals appear here on one crystal only. A defect goes right through the crystal plate and a pair of spirals develops simultaneously, one on the back and one on the front of the plate, from this common defect. Spiral steps measured interferometrically exhibit unusual anomalies which are discussed.

It is well known that a large proportion of even the best-formed silicon carbide crystals hitherto examined exhibit notable growth spirals on the basal pinacoid. These have been studied by many investigators, notably Verma (1951), Amelinckx (1951) and others. Not only have spiral growths been established, but in addition a variety of step heights have been evaluated by using the precision techniques of multiple-beam interferometry. It is now well known that these spiral growths afford a most comprehensive confirmation of the dislocation theory of growth put forward by Burton, Cabrera & Frank (1949) and later more extensively developed especially by Frank (1951).

Most silicon carbide crystals exhibit some colour, varying from a light shade of green, through to a brilliant black. Through the courtesy of Dr Knippenberg of Phillips, Eindhoven, we have available a collection of extremely pure crystals of silicon carbide. These were received as an incrustation of transparent colourless thin crystal plates (some hundreds), growing out towards the centre from an annular ring of friable graphite. The crystals (many of them several millimetres across) were all beautifully formed and each was clearly a single crystal, all being notable for their transparency and complete absence of any colour. They were clearly of much higher purity than the usual commercial silicon carbide crystals.

Since spiral growth formation is certainly linked to the presence of severe dislocation, and as included

impurities must clearly encourage development of such screw dislocations, it was suggested to us by S. Tolansky that there was a considerable likelihood that these very pure silicon carbide crystals might indeed not exhibit any spiral growths at all, in contradistinction to the usual run of silicon carbide crystals. We have therefore carried through a multiple-beam interferometric study of the surface microtopographies of over a hundred of these pure crystals and this report summarizes the findings. The crystals studied were mostly of similar thickness, transparent plates of the order of a quarter of a millimetre thick, all plane, and exhibiting well developed pinacoid (0001) faces. In accordance with standard practice in this laboratory (Tolansky, 1948) the crystals were silvered (reflectivity >95%) and examined, first by phase contrast, then with multiple-beam Fizeau fringes (green mercury source) and in selected cases with white-light fringes of equal chromatic order. In specific instances information was obtained without silvering, and at times by the use of polarized light.

### Observations

With one single and obviously an unusual exception, our examination of over 100 crystals failed to reveal any spiral growths at all. Now evidence has long since accumulated that the familiar spirals on silicon carbide have step heights normally several integral multiples